Modeling and estimation of deformation behavior of particle-reinforced metal-matrix composite

Tomita, Yoshihiro
Higa, Yoshikazu
Fujimoto, Takehiro

(Citation)
International Journal of Mechanical Sciences,42(11):2249-2260

(Issue Date)
2000

(Resource Type)
journal article

(Version)
Accepted Manuscript

(URL)
https://hdl.handle.net/20.500.14094/90000033

MODELING AND ESTIMATION OF DEFORMATION BEHAVIOR OF PARTICLE REINFORCED METAL-MATRIX COMPOSITE

Yoshihiro TOMITA*, Yoshikazu HIGA* and Takehiro FUJIMOTO**

Tel: +81-78-803-6125 Fax: +81-78-803-6155
tomita@mech.kobe-u.ac.jp http://solid.mech.kobe-u.ac.jp
*Graduate School of Science and Technology, Kobe University,
Rokkodai, Nada, Kobe, 657-8501 JAPAN
**Graduate School, Kobe University of Marchant-Marine

Abstract

In order to estimate the characteristic feature of the deformation behavior of materials with a length scale, the strain gradient plasticity theories, corresponding variational principle and a finite element method are given. Then the finite element method is applied to the estimation of the mechanical characteristics of the particle reinforced metal-matrix composites modeled under plane strain conditions. The effects of the volume fraction, size and distribution pattern of the reinforcement particles on the macroscopic mechanical property of the composite are discussed. It has been clarified that the deformation resistance of the composite is substantially increased with decreasing particle size under a constant volume fraction of the reinforcement material. The main cause of the increase of the deformation resistance in the plastic range is the high strain gradient appearing in the matrix material, which increases with the reduction of the distance between particles.

Corresponding Address:

Yoshihiro TOMITA
Department of Mechanical Engineering
Faculty of Engineering, Kobe University
Nada, Kobe, 657-8501 JAPAN
Tel: +81-78-803-6125 Fax: +81-78-803-6155
tomita@mech.kobe-u.ac.jp http://solid.mech.kobe-u.ac.jp

1. Introduction

Understanding the mechanism of plastic flow and the associated phenomena of patterning and localization of plastic deformation into shear bands is essential for the modeling and estimation of the mechanical properties of the materials that depend on the characteristic length scale. Research related to the phenomena that depend on the characteristic length of the microstructure of the materials can be traced back to the research concerning the Cosserat material and materials with length scales[1,2]. However, studies employing the generalized constitutive equation with a length scale that accounts for the microstructural interaction and evolution of microscopic texture find their roots in the pioneering work done by Aifantis [3][4] and Fleck et al. [5]. In the former, resulting constitutive equations contain the higher order terms of the strain gradient [3][4], whereas, in the latter, the constitutive equation [5] contains the first gradient of strain, which is derived from the geometrically necessary dislocation [6]. The related review and the details of the origin of the strain-gradient-dependent nature of the deformation behaviors have been extensively discussed [7,8]. Subsequently, the length-scale dependence of the localized zone and internal structures has been characterized using the constitutive equations based on the strain gradient plasticity theories [9-14]. Furthermore, it has been clarified that regularization with strain gradient plasticity theories substantially reduces the mesh dependence of the results obtained by finite element methods [15-17], which is well accepted in the field of computational mechanics. Thus, the strain gradient theory seems to provide a direct means of modeling the size effect of plastic flow within a continuum mechanics approach.

In this paper, the strain gradient plasticity theory and related variational principles, the computational frameworks for the simulation of plastic deformation behavior of materials obeying strain-gradient-dependent flow stress, are given. Then the finite element method is applied to the estimation of the mechanical characteristics of the metal-matrix composites under plane strain conditions. The mesh sensitivity of the computationally predicted results and the effects of the volume fraction, size and distribution pattern of the reinforcement particles on the macroscopic mechanical property of the composite are discussed.

2. Strain Gradient Plasticity Theory

To indicate the constitutive equation an updated Lagrangian formulation is employed, wherein each material particle is labeled by a coordinate x_i. For elasto-plastic solids, the symmetric part of the deformation rate gradient D_{ij} is assumed to be decomposed into an elastic part D_{ij}^e and a plastic part D_{ij}^p. Then, we have the relation

$$D_{ij} = D_{ij}^e + D_{ij}^p . \tag{1}$$

An elastic response is assumed to be isotropic and to be expressed by Hooke's law [18]:

$$\hat{S}_{ij} = \hat{\sigma}_{ij} + \sigma_{ij} D_{kk} = C_{ijkl}^e D_{kl}^e , \tag{2}$$

$$C_{ijkl}^e = 2G\left\{ \frac{1}{2}\left(\delta_{ik}\delta_{jl} + \delta_{il}\delta_{jk}\right) + \frac{\nu}{1-2\nu}\delta_{ij}\delta_{kl} \right\},$$

where G is the elastic shear modulus, ν is Poisson's ratio and $\hat{S}_{ij}$, $\hat{\sigma}_{ij}$ are the Jaumann rates of Kirchhoff stress S_{ij} and Cauchy stress σ_{ij} in the current state, respectively.

Next, a constitutive equation for the plastic strain rate D_{ij}^p with strain gradient dependence is indicated, with the help of Mises type flow rule, as

$$D_{ij}^p = \frac{3\dot{\varepsilon}}{2\sigma}\sigma'_{ij} ,$$

$$\sigma = \left(\frac{3}{2}\sigma'_{ij}\sigma'_{ij} \right)^{1/2} , \quad \dot{\varepsilon} = \left(\frac{2}{3} D_{ij}^p D_{ij}^p \right)^{1/2} , \tag{3}$$

where σ'_{ij} is a deviatoric part of Cauchy stress, σ is the equivalent stress and $\dot{\varepsilon}$ is the equivalent plastic strain rate.

The yield function for the strain-rate-independent materials becomes

$$f = \sigma - \overline{\sigma} = 0 \tag{4}$$

The strain-gradient-dependent flow stress $\overline{\sigma}$ can be expressed along the same lines, as indicated by Zbib and Aifantis[9].

$$\overline{\sigma} = \overline{\overline{\sigma}}(\varepsilon) - c\varepsilon_{,ii} \tag{5}$$

Where, $\overline{\overline{\sigma}}(\varepsilon)$ is the conventional work hardening function and the second term indicates the strain-gradient-dependent terms. c is the coefficient describing the degree of dependence on the strain gradient. Further discussions on more elaborate constitutive equations are given by Zbib and Aifantis[9]. With Eqs.(4) and (5), the

consistency condition $\dot{f} = 0$ becomes

$$\dot{\sigma} - \dot{\overline{\overline{\sigma}}} + c\dot{\varepsilon}_{,ii} = 0 . \tag{6}$$

Combining Eqs. (1), (2) and (3), we derive the elasto-plastic constitutive equation

$$\hat{S}_{ij} = C^{e}_{ijkl}\left(D_{kl} - \frac{3\dot{\varepsilon}}{2\sigma}\sigma'_{kl} \right). \tag{7}$$

The equivalent strain rate $\dot{\varepsilon}$ is calculated from Eq. (6). Thus, the equivalent strain rate $\dot{\varepsilon}$ can be treated as an independent variable; as a result, the variational principle, as will be indicated in the next section, becomes very simple and the finite element equation with a conventional C^0 element can be established[18].

The derivation of the constitutive equation for the strain-rate-dependent material with strain gradient dependence is straightforward. The corresponding expression is Eq. (5) in which the flow stress has been replaced by the strain-rate-dependent one.

$$\overline{\sigma} = \overline{\overline{\sigma}}(\varepsilon, \dot{\varepsilon}) - c\varepsilon_{,ii} \tag{8}$$

The constitutive equation for elasto-viscoplastic materials becomes Eq.(7). The corresponding expression of Eq. (7) for a materials with temperature dependence can be derived by replacing the flow stress in Eq.(8) by the temperature-dependent one [15,19,20].

3. Variational Principle and Finite Element Method

In this section, the variational principle for materials obeying the above described constitutive equation is discussed and the associated additional boundary condition is derived. Consider a body with volume V and surface S subjected to a velocity constraint on S_v and traction rate on S_t. The weak form of the equilibrium equation and compatibility condition Eq.(6) is

$$\int_V \left(\dot{S}_{ij} + \sigma_{mj} v_{i,m} \right) \delta v_{i,j} dV - \int_{S_t} \dot{P}_i \delta v_i dS + \int_V \left(\dot{\sigma} - \dot{\overline{\overline{\sigma}}} + c\dot{\varepsilon}_{,ii} \right) \delta\dot{\varepsilon} dV = 0 , \tag{9}$$

where $\dot{P}_i$ is the prescribed surface traction rate on the boundary S_t and v_i is velocity. δv_i is the virtual velocity satisfying the homogeneous boundary condition over S_v. $\delta\dot{\varepsilon}$ is the variation of equivalent strain rate. We employ the divergence theorem to reduce the order of the derivative of the equivalent strain rate and arrive at the reduced

equation

$$\int_V \left(\dot{S}_{ij} + \sigma_{mj} v_{i,m}\right) \delta v_{i,j} dV - \int_{S_t} \dot{P}_i \delta v_i dS + \int_V \left\{\left(\dot{\sigma} - \dot{\bar{\sigma}}\right) \delta\dot{\varepsilon} - c\dot{\varepsilon}_{,i} \delta\dot{\varepsilon}_{,i}\right\} dV = 0, \qquad (10)$$

$$c n_i \dot{\varepsilon}_{,i} = 0 \quad \text{on} \quad S, \qquad (11)$$

where n_i is the unit normal of the surface S. The first two terms of Eq. (10) are the weak form of the equilibrium equation for conventional materials [18]. The subsequent term corresponds to the compatibility equation. Eq.(11) describes the additional boundary condition for $\dot{\varepsilon}$ on the surface S that appears due to the introduction of the strain gradient term[12,21]. This equation indicates the vanishing condition of strain rate flux through the surface S. When $c = 0$, the above-mentioned variational principle becomes the variational principle for a material obeying conventional elasto-plastic constitutive equation [18].

Next, finite element methods for materials obeying strain-gradient-dependent constitutive equation will be derived based on the variational principle above obtained. The variables subjected to variation are velocity v_i and equivalent strain rate $\dot{\varepsilon}$, the maximum derivative of which in Eq. (10) is of the first order so that the finite element with C^0 continuity can be used. As a result, variables v_i, $\dot{\varepsilon}$ and their gradients $v_{i,j}$, $\dot{\varepsilon}_{,i}$ may be expressed using the shape function ϕ_N and its gradient $\phi_{N,i}$, and the nodal values of variables v_{Ni} and $\dot{\varepsilon}_N$ at node N. Substituting these relations into Eq.(10) and after some manipulation, we can obtain the finite element equation for an element.

$$K^1_{NiMk} v_{Mk} + K^2_{NiM} \dot{\varepsilon}_M = \dot{f}_{Ni} \qquad (12)$$

$$K^2_{NiM} v_{Ni} + K^3_{NM} \dot{\varepsilon}_M = 0$$

Where the matrices K^1_{NiMk}, K^2_{NiM} and K^3_{NM} are the conventional stiffness matrix, the matrix correlating the interaction between the nodal velocity and the nodal equivalent strain rate, and the matrix representing the stiffness for the nodal equivalent strain rate, respectively. Furthermore, $\dot{f}_{Ni}$ is the equivalent nodal force vector. The concrete form of these matrices has been shown by Fujimoto [22]. By using the compatibility condition of nodal velocities and equivalent strain rates, and the equilibrium condition of nodal forces, the stiffness equation for the entire system can be established. It should be noted that the equivalent strain rate on the surface must satisfy a condition (11). A

more extended version for the dynamical problems and the discussion concerning the accuracy of the conventional finite element method with strain-gradient-dependent constitutive equation (7) have been given by Tomita and Fujimoto [20].

4. Characteristic Feature of Metal-Matrix Composites

There has been a great deal of effort directed towards understanding the relationship between the microstructure and mechanical behavior in particulate reinforced matrix composites, as briefly summarized by Zhu et al. [23]. For relatively large reinforcement particles of micrometer size and larger, continuum plasticity formulations are used, and it has been clarified that the deformation behavior is affected by the volume fraction but is independent of particle size. However, experimental results [24] suggest that the yield stress of a particl-reinforced Al matrix composite depends on both the volume fraction and particle size. Recently, a continuum model has been developed [13] for the viscoplastic deformation in metal-matrix composites, utilizing a finite unit cell comprised of rigid ellipsoidal inclusions surrounded by a matrix metal, and the effect of particle size on the flow strength of a composite has been clarified by employing the frameworks of Kroner [25] and Hill [26] with their strain gradient constitutive equation. However, their approaches are based on the theory in which the ellipsoidal inclusion is assumed in an infinite region so that the interaction between the inclusions in the high-volume-fraction cases and the effects of shape and distribution pattern are not clarified; therefore, the computational simulations described herein are indispensable.

Here, the problems associated with the size- and distribution-pattern-dependent macroscopic strength of the metal-matrix composites are investigated by employing the strain-gradient-dependent constitutive equations and the above-described finite element method. The distribution of the reinforcement particles and their shapes are assumed to be fixed and the unit cell shown in Fig.1 is employed for the finite element simulation. The boundary conditions for the unit cell are such that the upper and bottom surfaces are shear free with a constant displacement constraint, whereas the right and left surfaces are assumed to be displaced by a constant amount along the x direction, the magnitude of which is determined such that the total x directional force vanishes. For comparison purposes, two different particle distribution patterns, shown in Fig.2, are

introduced. In all cases, due to the symmetric deformation with respect to x and y directions, one-quarter of the cell is calculated. The effects of volume fraction, size and the pattern of distribution of particles on the macroscopic behavior of the composites are investigated through computational simulation.

Since the present investigation focuses on the effect of the strain gradient terms in the constitutive equation for matrix materials on the macroscopic deformation behavior of particle reinforced-composites, a very simple constitutive equation for the plastic deformation of matrix material is assumed, $\bar{\bar{\sigma}} = \sigma_y \left(1 + \varepsilon / \varepsilon_0\right)^n \left(1 + \dot{\varepsilon} / \dot{\varepsilon}_0\right)^m$, with material constants $\sigma_y = 275MPa$, $\varepsilon_0 = 0.002$, $\dot{\varepsilon}_0 = 0.002/s$, $n = 0.25$ and $m = 0.024$, elasticity modulus $E = 69.0GPa$ and Poisson's ratio $\nu = 0.333$. The coefficient of the strain gradient was set to be $c = 360\sigma_y l^2$, $l = L/16$. The reinforcement particles are assumed to be elastic with elasticity modulus $E = 450GPa$ and Poisson's ratio $\nu = 0.170$.

In this investigation, finite element simulations have been performed for particulate-reinforced composites with different volume fractions of reinforcement, particle sizes and distribution patterns. Therefore, computational modes with different mesh sizes are indispensable, so that the effect of mesh size on the results of computational simulation should be checked before concrete discussion. In order to check the influence of finite element discretization on the predicted deformation behavior, computational models with 16x16, 24x24 and 32x32 discretization for x and y directions were used for the one-quarter region, as shown in Fig.4. Figure 3(a) indicates the average stress and strain relations for three different discretization models. The corresponding equivalent strain distribution and the area with the positive strain gradient term are shown in Fig.3(b). Almost identical average stress and strain relations, equivalent strain distribution and the area with positive strain gradient term are obtained with different finite element discretization models, which is well consistent with previously reported results for flow localization problems [15-17]. Consequently, as far as the present problems are concerned, the simulated results are independent of the finite element discretization size employed.

Figure 4(a) indicates the average stress and strain relations for the composites with different volume fractions of reinforcement particles, $V_f = 6.25$, 11.1 and 25.0%, with identical particle size $d = 12.0\,\mu\mathrm{m}$. The difference in the stiffness between the

matrix and particles is marked so that the deformation applied is absorbed by the soft matrix area, which causes a high strain gradient in the matrix area as indicated in Fig.4(b). Therefore, the strain gradient increases, as the volume fraction of the reinforcement particles increases, which results in the higher strength of the composite as compared with strain-gradient-independent materials.

Next, the effect of the size of the reinforcement particles on the strength of the composites is investigated with a constant volume fraction of reinforcement particles . Figure 5(a) shows the average stress and strain relation for the composites with a fixed volume fraction of reinforcement particles, $V_f = 25.0\%$, with different sizes, d=12, 14, 16, 18 and $20\,\mu$m. The stress-strain relations for the composites obeying strain-gradient-independent constitutive equation are identical, regardless of the size of the particles, and the distribution of the plastic equivalent strain is almost identical. On the other hand, the resistance to deformation increases as the size of the reinforcement particle decreases for a material obeying the strain-gradient-dependent constitutive equation. This tendency is caused by the increases in the strain gradient of the matrix as the particle size decreases, which can be clearly observed in Fig.5(b), and is consistent with the experimentally clarified evidence [24,27].

Lastly we will discuss the effect of the distribution patterns of the reinforced particles, as shown in Fig.2, on the deformation behavior of composites. The volume fraction is fixed at $V_f = 25.0\%$ and the size of the reinforcements is $d = 12.0\,\mu m$. Figures 6(a) and (b) show the average stress and strain relations and the plastic equivalent strain distribution, respectively. Considerable differences in average stress and strain relations for different distribution patterns are seen. The square distribution pattern of reinforcement particles has a tendency to increase the deformation resistance more than the triangular pattern. This may be explained by the plastic equivalent strain distribution. That is, the size of the band like regions such as the high strain region emanating from the particle and matrix boundary which strongly related to the particle distribution, affect the difference observed in the resistance of the composites.

5. Conclusion

In this investigation, we discussed the variational principle for materials obeying strain gradient elasto-plastic constitutive equations and a simple finite element method.

Then, to reproduce the experimentally observed evidence for the particulate-reinforced composites which exhibit particle-size-dependent macroscopic characteristics, a simplified computational model employing the strain gradient constitutive equation for plastic deformation of the matrix material was developed.

Through a series of simulations with different finite element discretizations, it was clarified that the computationally predicted results exhibit the mesh-size independent feature. Subsequently, using the proposed simplified model of a particle-reinforced composite under plane strain conditions, the effects of the volume fraction, size and distribution pattern of reinforced particles on the macroscopic characteristic feature of the composites were clarified. The results indicated that the present simulation strategy has the capability of predicting the experimentally observed particle-size-dependent macroscopic characteristic feature of the composites. The main mechanism of the increase of the deformation resistance in the plastic range is attributable to the high strain gradient in the matrix material, which increases with decreasing the distance between the particles.

To directly compare the results predicted by computational simulation against those found experimentally, we must identify the material parameters for the matrix and the reinforcement particle, as well as the coefficient which determines the effect of the strain gradient term on the flow stress of the matrix material under a high strain gradient.

Acknowledgment: Financial support from the Ministry of Education of Japan is gratefully acknowledged.

References

1) K. Kroner, Elasticity theory of materials with long range cohesive forces, Int. J. Solids Struct., **3**, 731(1967).

2) A. C. Eringen, Linear theory of nonlocal elasticity and dispersion of plane waves, Int. J. Engng. Sci., 10, 425 (1972).

3) E. C. Aifantis, On the microstructural original of certain inelastic models, Trans. ASME, Eng. Mat. Tech. **106**, 326-330 (1984).

4) E. C. Aifantis, The physics of plastic deformation, Int. J. Plasticity, 3, 211-247(1987).

5) N. A. Fleck, G. M. Muller, M. F. Ashby and J. W. Hutchinson, Strain gradient plasticity: Theory and experiment, Acta Metall. Mater., **42**, 475-487 (1994).

6) M. F. Ashby, The deformation of plastically non-homogeneous alloys, In Strengthening Methods in Crystals, A. Kelly and R. B. Nicholson eds., 184 (1971), Elsevier, Amsterdam

7) E. C. Aifantis, Spatio-temporal instabilities in deformation and fracture, In Computational Material Modeling, A. K. Noor and A. Needleman eds, AD-Vol.42/PVP-Vol.294, ASME, 199-222 (1994).

8) H. M. Zbib and E. C. Aifantis, A gradient-dependent plasticity theory of plasticity, Appl. Mech. Rev., ASME, **42** ,295-304(1989) .

9) H. M. Zbib and E. C. Aifantis, On the localization and postlocalization behavior of plastic deformation, Part I, On the initiation of shear band, Res. Mechanica, **23**, 261(1988).

10) H. M. Zbib and E. C. Aifantis, On the localization and postlocalization behavior of plastic deformation, Part II, On the evolution and thickness of shear band, Res. Mechanica, **23**, 279(1988).

11) H. M. Zbib and E. C. Aifantis, On the localization and postlocalization behavior of plastic deformation, Part III, On the structure and velocity of the Parterin-Le Chatelier bands, Res. Mechanica, **23**, 293(1988).

12) H. M. Zbib, Size effect and shear banding in viscoplasticity with kinematic hardening, Materials Instabilities, Theory and Applications, R.C.Batra and H. M. Zbib eds, AMD-Vol.183/MD-Vol.50, ASME 19(1994).

13) H T. Zhu, H. M. Zbib and E. C. Aifantis, Flow strength and size effect in metal matrix composite, AMD-Vol.202/MD-Vol.61, Micromechanics and Constitutive

Modelling of Composite Mat. ASME, No.11, 103(1995).

14) I. Vardoulakis and E. C. Aifantis, A gradient flow theory of plasticity for granular materials, Acta Mechanica, **87** ,197-217(1991).

15) Y. Tomita, Simulation of plastic instabilities in solid mechanics, Appl. Mech. Rev., **47**, 171(1994).

16) Y. Tomita and T. Nakao, Shear localization in thermo-elasto-viscoplastic plane strain blocks, IUTAM Symposium, Finite Inelastic Deformations, Theory and Applications, D. Besdo and E. Stein eds. Hannover, Germany, 19 (1991).

17) Y. Tomita, Computational Approaches to plastic instability in solid mechanics, Theoretical and Applied Mechanics 1992, S. R. Bodner, J. Singer, A. Solan and Z. Hashin eds. 81(1993), Elsevier Science Publishers B.V.

18) Y. Tomita, Computational Elasto-Plasticity (1990) Youkendo (in Japanese)

19) Y. Tomita, Flow localization in plane-strain thermo-elasto-viscoplastic blocks under high rate of deformation Modelling Simul. Mater.Sci. Eng., **2** , 701(1994).

20) Y. Tomita and T. Fujimoto, Plane strain flow localization in tension blocks obeying strain-gradient-dependent constitutive equation M.S.R. Int., **1**, 254(1995).

21) H. B. Muhlhaus and E. C. Aifantis, A variational principle for gradient plasticity, Int. J. Solids Struct. **28**, 845-858 (1991).

22) T. Fujimoto, Computational estimation of flow localization and strength of ductile materials, Ph.D thesis, Kobe University (1997)

23) H-T. Zhu, H.M.Zbib and E.C.Aifantis, Flow strength and size effect in metal matrix composites, AMD-Vol.202/MD-Vol.61, Micromechanics and Constitutive Modelling of Composite Materials, H.M.Zbib, I.Demir, H.-T.Zhu eds. ASME (1995) 103-115.

24) S. V. Kamat, J.P.Hirth and R. Mehrabian, Mechanical Properties of Particulate Reinforced Aluminium-Matrix Composites, Acta Metall. Mater., 37, 2395 (1991)

25) E. M. Kroner, Zur Plastischen Verformung des Vielkristalls, Acta Metall.,**9**, 155-161 (1961).

26) R. Hill, Continuum micro-mechanics of elastoplastic polycrystals, J. Mech. Phys. Solids, **13**, 89-101 (1965).

27) S. Ushigome, K. Yamamoto and K. Fukuda, Mechanical properties of SiC particle reinforced aluminium alloy composite, Steels and Iron,**75**, 1549 (1989) (in Japanese).

Figure Captions

Figure 1 Computational model of particle reinforced composite material with distribution pattern A in Fig.2 and volume fraction of reinforcement particles $V_f = 25.0\,\%$. $L = 12\mu m$, $d = 12\mu m$

Figure 2 Distribution patterns A and B of reinforcement particles.

Figure 3 (a) Average stress and strain relations estimated by finite element discretization meshes of 16x16, 24x24 and 32x32 and (b) equivalent plastic strain distribution (left) with contour interval of 0.02 and area with positive strain gradient term $-c\nabla^2\varepsilon/\sigma_y \geq 0.2$ (dark area on the right).

Figure 4 (a) Average stress and strain relations for composites with volume fraction of reinforcement particles V_f = 6.25, 11.1, 25.0% and particle size $d = 12\mu m$ and (b) equivalent plastic strain distribution (left) with contour interval of 0.02 and area with positive strain gradient term $-c\nabla^2\varepsilon/\sigma_y \geq 0.2$ (dark area on the right).

Figure 5 (a) Average stress and strain relations for composites with particle sizes d = $12,14,16,18,20\mu m$ and volume fraction of reinforcement particles $V_f = 25\%$ and (b) equivalent plastic strain distribution (left) with contour interval of 0.02 and area with positive strain gradient term $-c\nabla^2\varepsilon/\sigma_y \geq 0.2$ (dark area on the right).

Figure 6 (a) Average stress and strain relations for composites with distribution patterns A and B of reinforcement particles indicated in Fig. 2 and volume fraction of reinforcement particles $V_f = 25\%$ with size $d = 12\mu m$ and (b) equivalent plastic strain distribution (left) with contour interval of 0.02 and area with positive strain gradient term $-c\nabla^2\varepsilon/\sigma_y \geq 0.2$ (dark area on the right).

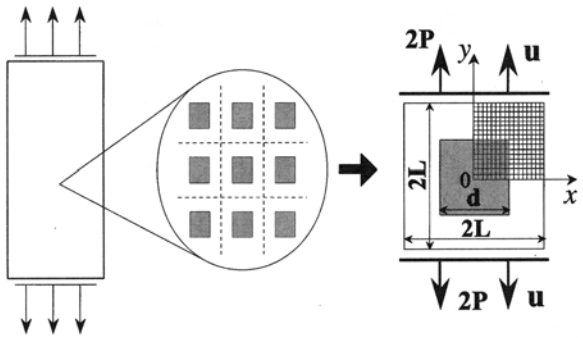

Figure 1.

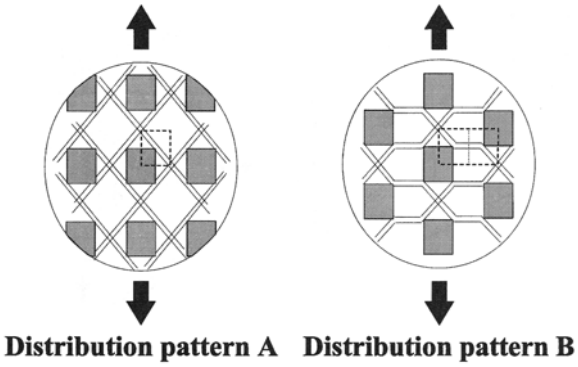

Figure 2.

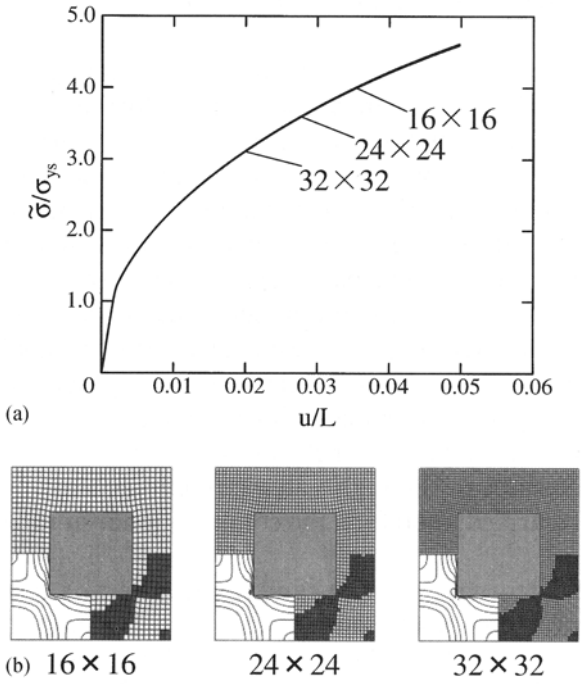

Figure 3.

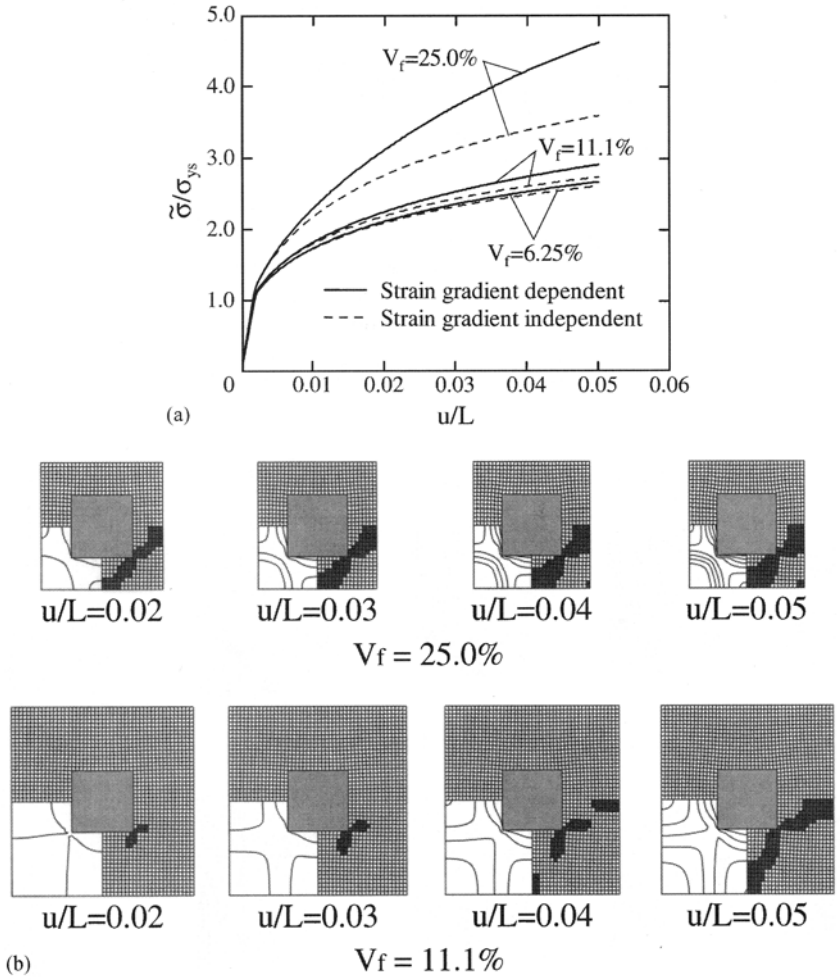
5.0
4.0
3.0
2.0
1.0
0
0.01
0.02
0.03
0.04
0.05
0.06
$\tilde{\sigma}/\sigma_{ys}$
u/L
V_f=25.0%
V_f=11.1%
V_f=6.25%
Strain gradient dependent
Strain gradient independent
(a)
u/L=0.02
u/L=0.03
u/L=0.04
u/L=0.05
Vf = 25.0%
u/L=0.02
u/L=0.03
u/L=0.04
u/L=0.05
(b)
Vf = 11.1%

Figure 4.

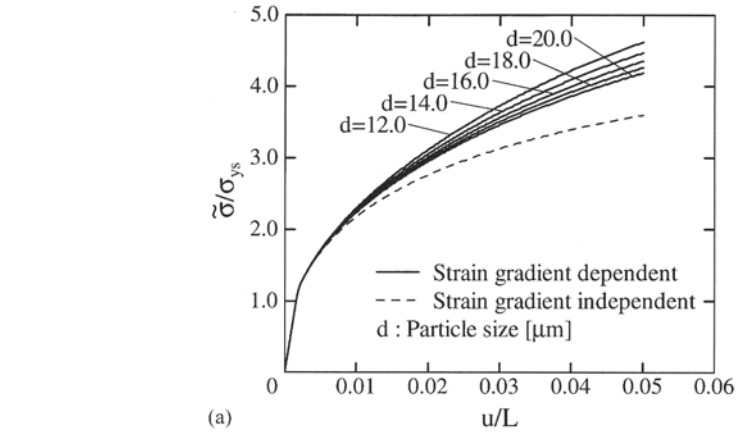

(a)

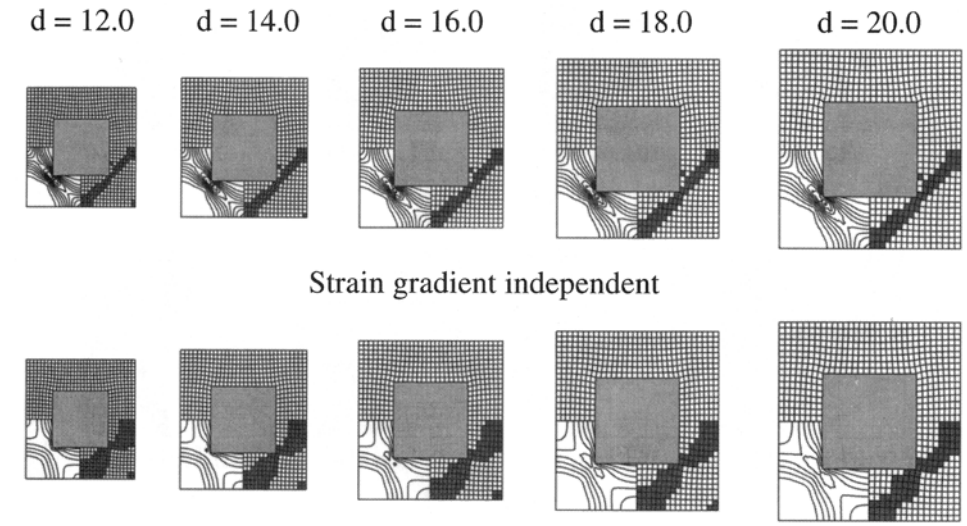

(b) d : Particle size [μm]

Figure 5.

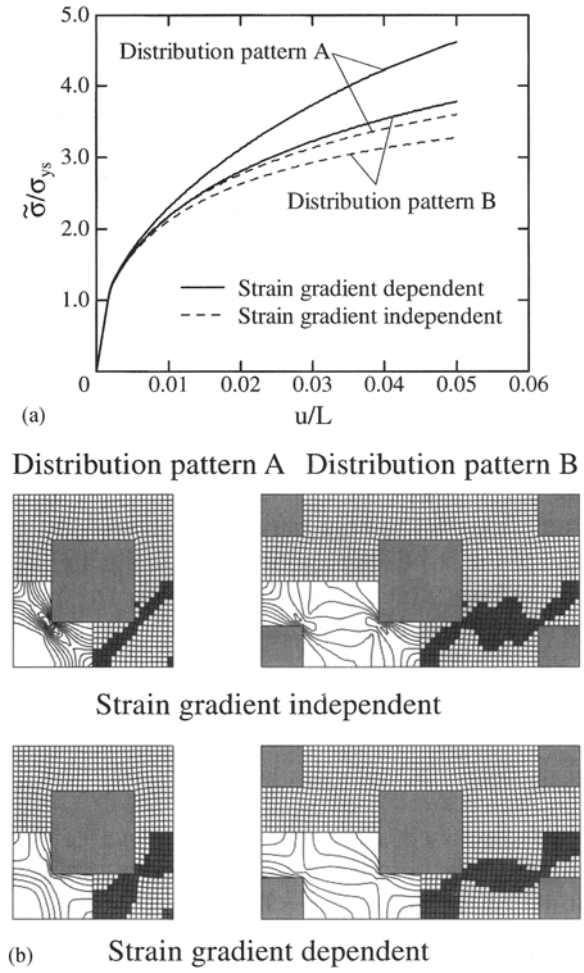
5.0
4.0
3.0
2.0
1.0
0
0.01
0.02
0.03
0.04
0.05
0.06
$\tilde{\sigma}/\sigma_{ys}$
u/L
Distribution pattern A
Distribution pattern B
Strain gradient dependent
Strain gradient independent
(a)
Distribution pattern A
Distribution pattern B
Strain gradient independent
(b)
Strain gradient dependent

Figure 6.